Title: The Heparan Sulfate Proteoglycan Syndecan-1 Influences Local Bone Cell Communication via the RANKL/OPG Axis

Short title: Syndecan-1 in local bone cell communication

Melanie Timmen[1,2], Heriburg Hidding[1], Martin Götte[3], Thaqif El Khassawna[4], Daniel Kronenberg[1, 2] and Richard Stange[1,2]

[1]Department of Regenerative Musculoskeletal Medicine, University Hospital Muenster, Germany;

[2]Institute of Musculoskeletal Medicine, University Hospital Muenster, Germany; [3]Department of Gynecology and Obstetrics, University Hospital Muenster, Germany; [4]Experimental Trauma Surgery, Justus-Liebig University Giessen, Germany

Corresponding Author:

Dr. rer. nat. Melanie Timmen,

Department of Regenerative Musculoskeletal Medicine

Institute of Muskuloskeletal Medicine

Westfaelische Wilhelms University Muenster

Albert Schweitzer Campus 1, D3

48161 Muenster, Germany

Tel.: +49-251-83 52682

Fax: +49-251-83 57025

e-mail: Melanie.Timmen@ukmuenster.de

Abstract

The cell surface heparan sulfate proteoglycan Syndecan-1 acts as a mediator of signals between the extracellular matrix and cells with high significance during pathogenesis. Besides binding a wide variety of molecules (e.g. growth factors, cytokines, matrix molecules) that play a role in essential cellular processes, Syndecan-1 is able to interact with OPG, one of the major regulators of osteoclastogenesis. Therefore, we investigated the influence of endogenous Syndecan-1 in murine osteoblastic and osteoclastic cells during local bone-cell-communication via the RANKL/OPG axis *in vitro and* the impact of Syndecan-1 deficiency on bone development and aging in an *in vivo* mouse model.

During aging, serum concentration of Syndecan-1 increased in wild type mice. On bone surfaces, expression of RANKL in osteocytes was more prevalent in aged Syndecan-1 deficient mice leading to higher numbers of osteoclasts. However, bone resorption appeared to be decreased in Syndecan-1 deficient mice. The potential of osteoblasts to induce osteoclastogenesis was characterized by a switch of OPG towards RANKL production and can be induced in osteoblasts by prostaglandin E2 and Vitamin D3. This switch also influenced Syndecan-1 expression on transcriptional and protein level. The lack of Syndecan-1 on osteoblasts in co-cultures of osteoblasts and osteoclast impaired the development of osteoclasts by changing cell-communication via the ratio of OPG and RANKL.

Syndecan-1 influences local bone cell communication during physiological bone remodelling. Syndecan-1 deficiency alters the release of OPG and RANKL by osteoblasts and osteocytes, and affects the differentiation of osteoclasts *in vitro* and *in vivo* in an age-dependent manner in healthy organisms. Syndecan-1 might therefore be of high impact as a new modulator of bone-cell-communication during bone regeneration or bone diseases where Syndecan-1 expression is known to be even more prevalent.

Keywords: Heparan sulfate proteoglycan (HSPG), Syndecan-1, osteoblast, osteoclast osteoprotegerin (OPG), aging

Introduction

Bone remodelling takes place throughout the whole life of a healthy organism. Micro damages within the bone or site-specific remodelling caused by changes of mechanical stimuli are sensed most likely by osteocytes, and a cascade of bone resorption and bone formation is started, mediated by so-called “basic multicellular units” (BMU) (1-3). Osteoclast precursors are targeted towards the site of remodelling by mostly unknown mechanisms. Nevertheless, it is known, that osteoclast differentiation is initiated by the *activation of receptor activator of nuclear factor -κB* (RANK) by its ligand RANKL. This is produced by osteocytes and osteoblasts, but also in bone marrow stromal cells and T-cells (4) in response to a variety of factors like *parathyroid hormone* (PTH), *parathyroid hormone related protein* (PTHrP), *tumour necrosis factor* (TNF)-alpha, *interleukin* (IL) -1-beta, *vitamin D3* ($1,25(OH)_2D_{3)}$ or *prostaglandin E2* (PGE2) (5, 6). Osteoblasts and osteocytes also produce osteoprotegerin (OPG), the soluble decoy receptor of RANKL, which binds to RANKL and thereby interferes with the osteoblast/osteoclast communication. Once resorption is terminated, osteoblast precursor cells are recruited to the site of action, where they differentiate to mature osteoblasts and deposit new bone material that is mineralized and fully functional with embedded osteocytes. The RANKL/OPG ratio determines the initiation and termination of osteoclastogenesis and with that the balance between bone formation and bone resorbtion.

Recently, some studies have drawn additional attention to heparan sulfate proteoglycans (HSPG) as new regulatory players of bone cell communication. It has been shown that isolated glucosaminoglycans (GAG) or heparin molecules stimulated osteoclastogenesis, and long term treatment with heparin lead to bone loss (7, 8). Heparanase over-expressing mice that produced higher levels of this GAG-cleaving protein, exhibited an increased bone mass (9). Recently, Nowaza *et al*. have pointed out, that the structure and sulfation of the heparan sulfate (HS) chains determined the interaction with OPG (10). They showed that mice deficient for *ext1 (a gene encoding exostosin glycosyltransferase-1,* an enzyme essential for the synthesis of HS chains), exhibited an osteopenic phenotype that was due to an enhanced osteoclast activity caused by decreased inhibition of OPG on RANKL. In contrast to RANKL, OPG has a heparin

binding domain and was shown to have a high affinity for GAGs (11). Especially in bone tumour development and metastasis, the interaction of proteoglycans like Syndecan-1 with OPG has been characterized (12). Proteoglycans were found in one complex together with RANKL/RANK and OPG, but heparin molecules also inhibited the binding of OPG to RANKL (7, 13). HS was identified as a component that caused a conformational change in OPG upon binding followed by dimerization of OPG which than resulted in an increased affinity of OPG to RANKL (14). Additionally, the immobilization of OPG at the cell surface via binding to membrane bound HSPG seemed to facilitate the interaction with membrane bound RANKL, and this inhibited osteoclastogenesis (10).

Syndecans, a family of four HSPG´s, are composed of an extracellular domain that contains up to three binding sites for GAG chains of different types, e.g. HS chains, some Syndecans also have chondroitin (CS) side chains, near the transmembrane domain (15). Additionally, the GAG chain composition is tissue specific, which influences the interaction with a high variety of ligands (16, 17). The extracellular domain can be shed from the cell surface at a well-characterized site close to the transmembrane region. Intracellularly, Syndecan proteins show a small cytoplasmic domain consisting of a variable domain flanked of two conserved domains that are responsible for intracellular signalling and interaction with the cytoskeleton.

Syndecans are known to be expressed in many different cell types at low levels, but also in a differentiation dependent manner (18). These proteins were shown to be up regulated during pathological processes (e.g. inflammation, cancer, healing processes, infection) and seemed to have an important function, there. The deficiency of Syndecan-1 led to higher mortality or more severe progression of many diseases (see review: Teng et al, 2012 (19)), but no obvious phenotype could be observed in an unchallenged organism (20). These findings are similar to recent findings of our research group regarding Syndecan-4, another member of the Syndecan family (21).

Sanderson *et. al.* (2004) and Velasco *et. al.* (2010) have summarized the results of several studies that investigated the role of proteoglycans and Syndecan-1 during osteolytic tumour growth and metastasis (13, 16). It was shown that Syndecan-1 is upregulated during a variety of

cancers (17, 22, 23). Recently, in multiple myeloma patients, high serum concentrations of Syndecan-1 have been recognized to influence osteoclastogenesis via OPG binding in bone metastases (12).

So far the influence of Syndecan-1 on bone structure or bone cell-cell communication under physiological conditions like bone development, bone homeostasis and aging has not been characterized. Although, because of its known interaction with OPG, Syndecan-1 seems to be a potential candidate to influence bone cell communication and bone remodelling. In this study, we investigated the influence of endogenous Syndecan-1 in murine osteoblastic and osteoclastic cells during local bone-cell-communication via the RANKL/OPG axis *in vitro and* the impact of Syndecan-1 deficiency on bone development and aging in an *in vivo* mouse model.

Methods:

Mice

All experiments were performed according to the protocol approved by the Landesamt für Naturschutz, Umweltschutz und Verbraucherschutz (LANUV, AZ: 84-02.05.50.A15.005), Northrhine-Westphalia, Germany according to the legislation for the protection of animals used for scientific purposes (Directive 2010/63/EU). C57Bl/6 Syndecan-1-/- (Sdc1-/-) mice were generated by Stepp *et. al.* (20, 24). All mice were inbred homozygously at a C57BL/6 genetic background. Mice were kept under conventional not pathogen-free conditions with a 12 hour light/dark cycle, up to 65% relative humidity and 20°C temperature in open cages grouped with up to 4 animals enriched with nesting material and paper houses. Mice had access to tap water and standard rodent chow (Altromin GmbH, Lage, Germany) ad libitum. Syndecan-1 deficient mice showed no severe phenotype, are vital and fertile.

Serum concentrations of Syndecan-1

Serum samples of 4, 12 and 18 month old wild type and Syndecan-1 deficient mice were prepared from blood collected after cervical dislocation. The concentration of Syndecan-1 was determined using an ELISA Kit (Boster Biological Technology, Pleasaton, CA, USA). In serum of Syndecan-1 deficient mice, no Syndecan-1 was detectable, as expected, therefore only results

of wild type mice are shown.

Histomorphometry

Histological analysis of the bone phenotype was performed according the nomenclature of Dempster *et. al*. using bones of newborn, 4, 12 and 18 month old female mice (wild type, Sdc1-/-) as indicated (25). The whole skeleton of newborn mice was used for alcian blue/alizarin-red staining to visualize cartilaginous (blue) and mineralized (red) bone. Longitudinal sections of humerus, femur and tibia embedded in paraffin were used for histological quantification of limb development in detail.

Bone tissue samples (lumbar vertebra) of adult mice were fixed in 4% paraformaldehyde (PFA) at 4 °C for 12 h. The bones were embedded undecalcified in methylmethacrylate (Technovit® 9100, Heraeus, Wehrheim, Germany). Sections (5 µm thickness) were obtained through the sagittal plane and TRAP staining was performed using Acid Phosphatase, Leukocyte (TRAP) Kit (Sigma Aldrich). Cell sense dimensions 1.17 (Olympus, Hamburg, Germany) was used to determine osteoclasts as TRAP positive cells located at the bone surface. Fifth lumbar vertebrae of adult mice (4-18 month) were fixed, kept humid and analysed by µCT (Skyscan 1176, Bruker, Billerica, MA, USA) for mineralized bone structure. µCT scanning and analysis was performed with a voxel resolution of 9 µm according to standard guidelines (26). Cortical and trabecular bone were analysed via segmentation using manufactors software (DataViewer, CTvox, CTan). Thresholds for trabecular bone were defined by the Outsu method included in the software.

Cell culture

For *in vitro* experiments with osteoblasts and osteoclasts, primary precursors of wild type and Syndecan-1 deficient mice were isolated. Primary **osteoblast precursors** were isolated from the calvarias of newborn mice by sequential digestion (0.2 % dispase Grade II (Roche, Sigma-Aldrich, /collagenase Typ Ia, Sigma Aldrich, C-9891). Cells were seeded ($2x10^4$ cells/well) in 24-well plates in alphaMEM medium (Merck, Darmstadt, Germany, #F0925) plus 10 % FCS (Gibco, Thermo Fisher, Waltham, MA, USA, #10270), 2 mM L-glutamine (Sigma-Aldrich, Merck #59202C) and penicillin (100 U/ml)/streptomycine (100 µg/ml), supplemented with 0.2 mM L-ascorbic acid 2-phosphate (Sigma-Aldrich, #A8960) and 10 mM beta-glycerol phosphate,

Sigma-Aldrich, #G9422; =DM (Differentiation medium for osteoblasts without osteoclastogenic potential, see Table 1) as described previously (27). After 24 hours, the non-adherent cells were removed. Isolated osteoblasts were differentiated separately up to 25 days with medium changed every second day. Mineralization was visualized by von Kossa staining and quantified photometrically by Alizarin Red S staining. The **osteoclast precursors** were isolated from the bone marrow of 4-6 week old mice (femur/tibia) and seeded ($2x10^6$ cells/well) in 6-well plates (alphaMEM plus 10 % FCS, 2 mM L-glutamine and penicillin (100 U/ml)/streptomycin (100 µg/ml) supplemented with 50 ng/ml recombinant murine (rm) M-CSF (R&D, #416-ML). After 24 hours the non-adherent cells were collected, counted and added ($4x10^5$ cells/well) to the adherent osteoblast precursors for further co-cultivation in presence of DM-medium supplemented with 1 µM PGE2 Sigma-Aldrich, #P6532) and 10 nM $1,25(OH)_2D_3$ (Sigma-Aldrich, #D1530) (=DM+; Differentiation medium for osteoblasts with osteoclastogenic potential, see Table 1) (28). Under stimulation with $1,25(OH)_2D_3$ and PGE2 (DM+) osteoblastic cells increase their osteoclastogenic potential by upregulation of RANKL expression and downregulation of OPG expression (29). For separate culture and differentiation of osteoclasts, precursor cells ($1x10^5$ cells/well) were seeded in 96-well plates in DM medium supplemented with rmM-CSF (day 1-3: 50 ng/ml, day 4-7 30 ng/ml, R&D) and rmRANKL (50 ng/ml, R&D). Differentiation of osteoclasts was quantified, in co-cultures after removal of osteoblast layer, by counting the TRAP positive, multinucleated cells (Acid Phosphatase Leukocyte Kit (387 A), Sigma-Aldrich). Resorption was analysed using dentin chips. Cells were seeded on cleaned and sterilized dentin chips in 96-well ($1x10^5$ cells/well) and cultured in DM-Medium supplemented with rmM-CSF and rmRANKL for up to 9 days. Cells were removed after lysis by sonication and resorption pits were stained with Indian ink and visualized using a BX51 microscope (Olympus).

mRNA expression of RANK/RANKL/OPG and Syndecan-1 and detection of proteins in supernatant of cells

During cultivation of osteoblasts and osteoclasts separately, as well as in co-cultures, mRNA expression of Syndecan-1, RANK, RANKL and OPG was analysed by quantitative realtime PCR as well as secretion of molecules (OPG/RANKL, Syndecan-1) into the supernatant of the cells

were determined by ELISA (OPG/RANKL: R&D Systems, Bio-Techne GmbH, Wiesbaden-Norderstedt, Germany, Syndecan-1: Boster Biological Technology). RNA was isolated using RNeasy Micro Kit (Qiagen, Hilden, Germany) and the concentration and quality of the RNA were measured photometrically. Reverse transcription of the RNA into cDNA was performed according to the manufactures´ instructions (High-Capacity RNA-to-cDNA Kit, ThermoFischer Scientific). For quantitative realtime PCR, primers were used as indicated in Table 2. Besides Syndecan-1, we also determined the expression of the three other Syndecan genes during differentiation of osteoclasts and osteoblasts. HPRT expression was used as an internal housekeeping gene and results were normalised to day 0. Relative quantification was performed according to the ΔΔCT method.

Immunochemistry

Protein synthesis of Syndecan-1 was shown by immunocytochemistry using a polyclonal antibody against murine Syndecan-1 (CD138) clone 281-2 (1:50, rat anti-mouse, BD Pharmingen) in co-cultured cells after fixation with ice-cold 99% methanol and heparitinase III (2.4mIU/ml, Sigma-Aldrich, H2519-50UN)/ chondroitinase ABC Lyase (0.1U/ml, Sigma-Aldrich, C2905) treatment. Amplification and visualization was performed using secondary antibody (1:50, goat anti-Rat IgG, BD Pharmingen, Heidelberg, Germany) conjugated with biotin (visualised by using Vectastein ALP Kit, AK-5000, Vector Laboratories, Burlinggame, CA, USA) and analysed using a BX51 microscope and cell sense dimensions software (Olympus).

Immunostaining of OPG and RANKL in osteocytes was performed on lumbar vertebrae decalcified sections as described previously (30). Sections were incubated in the primary antibody solution overnight with Dako buffer (Agilent Technologies GmbH, Ratingen, Germany). RANKL detection was performed using rabbit polyclonal primary antibody (ab216484, Abcam, Cambridge, MA, USA) diluted in 1:100 ratio. OPG detection was performed using rabbit polyclonal primary antibody (ab73400, Abcam) diluted in 1:200 ratio. Antibodies were visualized using ABC-AP kit (AK5200, Vectastain ABC kit, Vector Laboratories). The slides were counterstained with silver nitrate to investigate the changes in RANKL and OPG activity in osteocyte bone vicinity. The slides were mounted with Vitro-Clud (R. Langenbrinck GmbH,

Emmendingen, Germany). Microscopy images were taken using Leica DM5500 photomicroscope equipped with a DFC7000 camera and operated by LASX software version 3.0 (Leica Microsystem Ltd., Wetzlar, Germany). Histomorphometry was performed using ImageJ (software version 1.52h, NIH, Bethesda, MD; http://imagej.nih.gov/ij). Bone area was calculated as described before (31). Cell counter plugin from ImageJ was used to count osteocytes. Total osteocyte number and numbers per group were calculated and normalized to trabecular bone area.

Determination of C-terminal telopeptide of type I collagen (CTX) as a parameter of bone resorbtion

An ELISA detecting the cross-linked C-terminal telopeptide of type I collagen was performed as instructed by the manufacturer (Wuhan USCN Business Co., Ltd., Houston TX, USA). Serum was obtained from mice at 4 to 18 months of age after cervical dislocation.

Statistics

Statistical analysis was carried out using GraphPad Prism version 6.07 for Windows, GraphPad Software, San Diego, California USA, www.graphpad.com). Different statistical tests (Kruskal-Wallis, Mann-Whitney-U, Holm-Sidak) were used dependent on the groups that are compared and are indicated in the legend of the figures. Results were considered significant with a p-value <0.05.

Results

Syndecan-1 concentration in serum samples of mice during aging

Syndecan-1 is used as a serum marker that is increased during various diseases. We therefore determined the concentration of soluble Syndecan-1 (CD138) in serum of healthy 4, 12 and 18 month old mice. As shown in figure 1, in the serum of 7 from 9 young mice no Syndecan-1 was detected. Two serum samples showed a positive detection with a concentration of 524 pg/ml and 734 pg/ml of Syndecan-1. The number of Syndecan-1 positive serum as well as the maximum values of Syndecan-1 concentrations increased with age. In serum of 12 month old mice, 9 of 13 samples were positive for Syndecan-1 with a mean of 384 pg/ml, samples showed

a maximal value 2094 pg/ml. Almost all 18 month old mice showed Syndecan-1 positive detection (8 of 9 samples) with highest mean value of 829 pg/ml and maximal values in three samples of up to 2274 pg/ml.

Skeletal remodelling of Syndecan-1 deficient mice during bone development and aging

Analysis of the whole skeleton of newborn mice revealed no difference in bone size or development, appearance of growth plates, bone mineralization or collagen content (Supplemental Fig. 1) between WT and Sdc1-/- mice. Furthermore, using µCT, we analysed structural parameters of vertebra bones during growth and aging in female Syndecan-1 deficient mice and age matched wild type animals. As shown in figure 2, the ratio trabecular bone volume/tissue volume (BV/TV) of lumbar vertebra of Syndecan-1 deficient mice of all age groups showed decreasing values for bone mass like in wild type mice during aging. Overall, no significant differences were found between the genotypes. However, it seems that the loss of trabecular bone in Syndecan-1 deficient mice was more pronounced (31.2% mean bone loss between 4 and 18 month, $p>0.01$, WT: 19.3%) and faster (lower BV/TV values in 12 month old animals (24.4% ± 3.40), compared to wild type (26.7% ± 3.27). Further parameters of bone structure (whole BV/TV, cortical thickness, trabecular number, trabecular separation, trabecular thickness) were determined as well, but also showed no significant differences between age matched genotypes (Supplemental data Table 1).

Syndecan-1 expression in osteoblasts and osteoclasts

Since our results suggested that Syndecan-1 has some impact on bone and bone cells, we further investigated the mRNA expression and presence of Syndecan-1 in osteoblasts and osteoclasts as well as the impact of the lack of Syndecan-1 on bone cell differentiation and communication *in vitro*.

During differentiation of osteoclasts in presence of rmRANKL, the mRNA expression of *Sdc1* increased significantly over time, while the expression of other Syndecans remained low (Fig. 3A). This is of importance, as Syndecan-2 has previously been shown to affect RANKL expression in bone marrow cells (32). In contrast to this, during osteoblasts differentiation (DM Medium) all four Syndecans (*sdc1-4*) were expressed at low levels and only slightly increased

during differentiation (Fig. 3B). Protein synthesis of Syndecan-1 could be detected by immunehistochemistry in osteoblastic (OB) as well as in osteoclastic (OC) cells (Fig. 3C) as shown in a co-culture system using medium with presence of $1,25(OH)_2D_3$ and PGE2 (DM+ medium). Strong Syndecan-1 positive staining was detected in mononuclear osteoclast precursor cells during early osteoclast differentiation as well as in mature, multinucleated osteoclasts. We could show (Fig. 3D), that osteoblastic cells, that were stimulated towards increased osteoclastogenic potential (DM+ medium), showed an increase in mRNA expression of *Sdc1* (DM: 1.7, DM+: 3.1, n=2) and a tendency to a higher release of Syndecan-1 protein into the supernatant (DM: 109.5pg/ml; DM+: 149.5pg/ml, n=2). The stimulation of osteoblastic precursor cells with PGE2 and $1,25(OH)_2D_3$ (DM+ medium) yielded in a different expression of RANKL and OPG as shown in figure 3E. WT cells showed an increased RANKL expression and released detectable amounts of RANKL protein into the supernatant of the cells. OPG mRNA expression was down regulated and less OPG can be detected in the supernatant of the cells. In contrast to that, Syndecan-1 deficient osteoblasts show less increase of RANKL mRNA expression but comparable OPG expression levels. But, no RANKL could be detected in the supernatant of osteoblasts stimulated with PGE2 and $1,25(OH)_2D_3$. OPG concentrations in the supernatant of Sdc-1-/- cells were comparable with wild type cells. It is important to know, that RANKL bound to OPG is not recognized by the ELISA, which we further demonstrated by OPG titration in supplemental figure 2. Addition of increasing amounts of OPG to constant amounts of RANKL prevented detection of RANKL by ELISA. This means conversely, that in supernatants of Syndecan-1 deficient osteoblasts no OPG free RANKL molecules can be detected although mRNA expression was induced.

Functional analyses of osteoblasts lacking Syndecan-1 revealed no differences in mineralization capacity of the extracellular matrix compared to wild type cells (Fig. 4A,B). Osteoclast differentiation seemed to be slightly retarded in Sdc1-/- cells showing lower numbers of big multinucleated cells, which was also consistent with less resorption (Fig. 3B).

RANKL and OPG release in co-cultures of osteoblasts and osteoclasts

Bone cell communication was analysed as the differentiation of osteoclast precursors into mature osteoclasts mediated by co-culture with RANKL and OPG producing osteoblasts. The stimulation of the osteoblasts to increase their osteoclastogenic potential was induced by the addition of 1,25$(OH)_2D_3$ and PGE2 (indicated as DM+), that is known to upregulate RANKL mRNA expression in osteoblasts. Co-cultured cells without 1,25$(OH)_2D_3$ and PGE2 show no osteoclast development. The presence of 1,25$(OH)_2D_3$ and PGE2 alone changes the osteoclastogenic potential of the osteoblasts. As shown in figure 5A, the presence of wild type osteoblasts in the co-cultures led to the development of mature osteoclasts of both wild type and Syndecan-1 deficient osteoclasts. In co-cultures with Syndecan-1 deficient osteoblasts, clearly decreased osteoclast development was observed (also see quantification in Fig. 5B). To analyze, if Syndecan-1 has impact on the communication molecules OPG and RANKL the release of these were determined in the supernatant of the different co-cultured cells (Fig. 5C). In co-cultures with WT osteoblasts, a high release of RANKL (WT/WT: d3: 216 pg/ml; d7: 620pg/ml) and low release of OPG (WT/WT: d3: 309pg/ml, d7: 219pg/ml) was determined. In comparison to that, co-cultures with Syndecan-1 deficient osteoblasts displayed lower amounts of RANKL (Sdc1-/-/WT: d3: 81 pg/ml; d7: 309 pg/ml) and high amounts of OPG release (Sdc1-/-/WT: d3: 1930 pg/ml; d7: 1948 pg/ml) into the supernatants. Again, one has to keep in mind that the detection of RANKL bound to its inhibitor by ELISA is prevented, so one should conclude, that although RANKL mRNA expression is increased low amounts OPG-free RANKL could be detected. The difference is further illustrated by the calculation of the RANKL/OPG ratio in figure 5C showing a shift in the balance from RANKL towards OPG in cultures with Syndecan-1 deficient osteoblasts that was highly significant at day 7 of the culture. mRNA expression studies of the corresponding genes of RANK, RANKL and OPG revealed no striking differences between the genotypes or cell types cultivated separately or in co-culture (see supplemental figure 3). The induction of RANK over time was much higher in the co-cultured cells than in separated osteoclastic cells differentiated in presence of rmRANKL (upper, right). RANK expression at low level was observed also in separated primary osteoblast cultures, which point to some contamination of the culture with macrophages that was not further investigated.

RANKL expression was low in unstimulated osteoblasts (DM) and absent in osteoclasts culture. In co-cultures, RANKL expression was increased as shown previously with osteoblasts stimulated with DM+. OPG gene expression is induced, although at relatively low level, in wild type and Syndecan-1 deficient osteoblasts cultivated in the absence of $1,25(OH)_2D_3$ or PGE2 (lower, left), while, as expected, OPG expression is suppressed under conditions that increase osteoclastogenic potential (lower, right).

Because osteocytes directly communicate with local bone precursor cells in BMU´s via OPG and RANKL, we stained for OPG- and RANKL-producing osteocytes (red) in the trabecular network of the lumbar vertebra (example pictures: Figure 6A). As shown in figure 6B (quantification), in young mice (4 month) lacking Syndecan-1 the numbers of RANKL- and OPG-positive osteocytes are lower (OPG: 173 ± 150 cells/mm^2; RANKL: 219 ± 125 cells/mm^2) compared to wild type (OPG: 455 ± 240 cells/mm^2; RANKL: 367 ± 346 cells/mm^2). In contrast to that, in aged mice (18 month), the number of OPG-positive osteocytes was higher in Sdc1-/- (456 ± 130 cells/mm^2) than in WT (308 ± 152 cells/mm^2), and the number of RANKL-positive osteocytes was even more increased (Syndecan-1-/-: 622 ± 265 cells/mm^2; WT: 255 ± 199 cells/mm^2). To analyze the consequence of local osteocyte expression of OPG and RANKL, we counted the number of osteoclasts on the surface of trabeculae in the vertebrae of 4 to 18 month old mice (Fig. 6C). This revealed comparable amounts of osteoclasts in young Syndecan-1 deficient (3.3 ± 1.4 OC/mm) and wild type mice (3.5 ± 1.5 OC/mm), but a significant increased number of osteoclasts in aged mice deficient for Syndecan-1 (5.1 ± 2.7 OC/mm, WT: 1.7 ± 1.2 OC/mm, $p<0.05$). This did not yield into an increased bone loss (see Fig. 2). Therefore, we determined C-terminal telopeptide of type I collagen (CTX) in serum of mice as a bone resorption parameter (Fig. 6D). This revealed no significant differences in young mice (WT: 10.4 ± 3.0 ng/ml; Sdc1-/-: 7.86 ± 3.4 ng/ml), but significant lower CTX values in 18 month old Syndecan-1 deficient mice (5.16 ± 1.5 ng/ml, $p<0.017$) compared to wild type (9.55 ± 3.2 ng/ml) pointing to decreased bone resorption although higher osteoclast numbers.

Discussion

Syndecan-1 has been shown to bind OPG via its proteoglycan side chains and thereby interferes with bone resorption during breast cancer and multiple myeloma (12, 33). Because osteoblast-osteoclast communication, in a healthy organism, is a process that takes place in a well-defined compartment called *basic multicellular unit* (BMU), we postulate an influence of Syndecan-1 on local bone cell communication via OPG interaction and modulating induction of osteoclastogenesis. Therefore, we characterized direct osteoblast/osteoclast communication *in vitro* and the bone structure of mice deficient for Syndecan-1 during bone development and aging.

First, we determined increasing levels of soluble Syndecan-1 in the serum of WT mice in the course of aging. This pointed to an induction of Syndecan-1 expression and release of soluble protein into the system. Increasing concentrations of serum Syndecan-1 due to diseases have been reported in different studies in humans and mice and Syndecans are often described as important regulators in challenged systems. However Syndecan-1 has never been analysed in healthy organisms because in the knockout mice no obvious phenotype has been described before. In line with that our studies revealed no striking phenotypical differences in Syndecan-1-/- mice compared to age matched wild type mice with regard to bone structure at birth until adulthood (<4month). Although in the course of aging (4 to 18 month), differences were not significant, on closer inspection, pace of bone loss tended to be faster as well as total bone loss was higher in the Syndecan-1 deficient mice.

Furthermore, we characterized expression and regulation of Syndecan-1 in osteoblasts and osteoclasts. Osteoclasts (wild type) revealed specific upregulation of Syndecan-1 during differentiation, and a slight retardation of differentiation and bone resorbing capacity in Syndecan-1 deficient cells. Sdc1-/- osteoblasts mineralized their extracellular matrix in a comparable way to wild type cells. Without any stimulation, Syndecan-1 as well as Syndecan-2, -3 and -4 were expressed in OB cells at comparable and low levels. From these results, we concluded, that OB as well as OC were not functionally impaired by the lack of Syndecan-1 although OC development was slightly retarded. Next, we investigated the communication of osteoblasts and osteoclasts with regard to osteoblast driven osteoclast stimulation referred to as

osteoclastogenic potential of the OB and revealed a former unknown regulatory function of Syndecan-1. First, we could show, that Syndecan-1 expression and protein production in OB was dependent on the culture conditions using $1,25(OH)_2D_3$ /PGE2 used as a stimulus of osteoclastogenic potential in osteoblasts. Besides stimulation of RANKL and repression of OPG, which was expected, Syndecan-1 also was induced. Second, in direct co-cultures of OB and OC of different genotypes the presence of Syndecan-1 was a prerequisite for OC differentiation. We could demonstrate that Syndecan-1 expression in OB determined the development of OC. This was independent of the genotype of the osteoclasts co-cultured with the osteoblasts. From that, we also concluded that no OC derived Syndecan-1 compensate for the lack of Syndecan-1 in OB during onset of bone cell interaction in our setting most likely due to low expression in OC precursor cells as we showed. Third, a lack of Syndecan-1 in the OB has led to a high amount of OPG in the supernatants of co-cultures that was not due to increased OPG mRNA expression. This surplus of OPG did not allow the induction of osteoclastogenesis in these cultures even though RANKL expression was induced comparably in all cultures. Benad-Mehner *et. al.* (2014) found similar results in breast cancer cell (MCF7) when Syndecan-1 was knocked down using siRNA (12). In these cells, the mRNA expression of OPG was upregulated and more OPG was released into the environment. In indirect co-culture, osteoclastogenesis was impaired as well as resorption what could be reversed by OPG neutralizing antibodies. In line with this, we concluded from our results that Syndecan-1 interacts with OPG via binding to the GAG side chains, what in return prevents OPG binding to RANKL and allows RANKL binding to RANK on osteoclast precursors. We postulate that the binding of OPG to the HS chains presented by Syndecan-1 supports cell-cell interaction to induce osteoclastogenesis. This mechanism was similarly supposed by Standal *et. al.* during multiple myeloma (33). They showed that Syndecan-1 expressing myeloma cells bind OPG followed by internalization and degradation of OPG. This points to a function of clearance for Syndecan-1 in this case.

To prove a relevance of our findings on Syndecan-1 function in bone cell communication *in vivo* we determined the amount of RANKL and OPG producing osteocytes in wild type and Syndecan-1 deficient trabecular bone and correlated this to the amount of osteoclastic cells on

the bone surface during aging of mice. Both, OPG and RANKL expression in osteocytes were dependent on the age of the animal and on the presence of Syndecan-1. Most strikingly, Syndecan-1 deficient trabecular bone showed the highest amounts of RANKL positive osteocytes in aged mice. These findings were supported by the osteoclast number on the bone surface that was significantly increased in aged Syndecan-1 deficient mice compare to wild type. In contrast, our measurements of bone structure did not reveal a striking bone loss. Taking into account, that our *in vitro* data concerning osteoclast differentiation pointed to a Syndecan-1 deficiency dependent delay in osteoclastogenesis, we analysed a serum parameter of bone resorption (CTX) in mice. This revealed a decrease in bone resorption in the aged Syndecan-1 deficient mice although the number of osteoclasts was increased. This data pointed to an additional significance of Syndecan-1 in osteoclast differentiation and activity that is currently under investigation.

Based on our *in vivo* and *in vitro* data we propose a model of Syndecan-1 function in the direct interaction of osteoblasts and osteoclasts to support the switch from bone formation to bone resorption (Fig. 7). Bone cell communication during bone formation leads to high OPG expression and release into the environment (Fig. 7A). Osteoblasts produce some low amount of Syndecan-1 and no/little amount of RANKL is released into the environment. Under these conditions, osteoclastogenesis is supressed by an excess of OPG that inactivates RANKL. Upon induction of bone resorption (Fig. 7B) induced by presence of $1,25(OH)_2D_3$/PGE2, by increase of inflammatory cytokines, stress conditions, aging and many more (34-37). These signals lead to a change in OPG and RANKL expression by OB and release into the environment. OPG expression is downregulated, RANKL expression is increased and RANKL binds to RANK at the surface of osteoclast precursor cells. Our data suggest Syndecan-1 to be an additional and significant component in this process. First, expression of Syndecan-1 is induced in osteoblasts with osteoclastogenic potential. Syndecan-1 molecules bind OPG, block OPG/RANKL interaction and with that promote RANKL stimulation of osteoclastogenesis. This function is suppressed if Syndecan-1 is missing (Fig. 7B, lower panel). Even if OPG expression is downregulated, OPG cannot be removed from the environment and inhibits RANKL and with

that osteoclastogenesis. In our setting, the genotype of the osteoblasts determined the fate of osteoclast development. This is supported by the findings of Nozawa *et al.* (2018), who have shown that OPG bound to HS on the surface of osteoblasts effectively contributed to the inhibition of RANKL interaction to RANK (10). Li *et. al.* proved that HS determined the conformation of OPG, its dimerization and with that the binding affinity to RANKL (14). In both studies, RANKL was considered a membrane bound receptor and OPG had to be arranged in a HSPG/OPG/RANKL complex at the osteoblast surface to effectively inhibit RANKL function. The impact of Syndecan-1 that is located on the surface of osteoblasts as well as the role of Syndecan-1 shedding from the surface of the osteoblasts is currently under investigation.

Conclusions

Our results provide evidence that Syndecan-1 acts as a modulator during cell-cell communication between osteoblasts and osteoclasts in bone homeostasis and in aging. Syndecan-1 is produced by osteoblasts that show osteoclastogenic potential and supports OPG clearance and RANKL binding to its receptor on osteoclast precursor cells. This function of Syndecan-1 might therefore be of high impact during bone regeneration processes or bone diseases.

Acknowledgements

Authors´ role: Study design: MT, RS; Study conduct: MT; Data collection: MT, HH, TK; Data analysis: MT, HH, TK; Data interpretation: MT; DK, RS; Drafting manuscript: MT, DK, RS; Revising manuscript content: MG, DK, RS; Approving final version of manuscript: MT, DK, RS; MT takes responsibility for the integrity of the data analysis.

We thank Simone Niehues, Nina Ehrens and Iska Loessmann for excellent technical assistance. Martin Goette kindly provided the Syndecan-1 deficient mouse strain.

This work was funded by the German Research Foundation (DFG, STA 650/4-0) and by 'Cells-in-Motion Cluster of Excellence' (EXC 1003 – CiM), University of Muenster, Germany.

References

1. Sims NA, Martin TJ. Coupling the activities of bone formation and resorption: a multitude of signals within the basic multicellular unit. Bonekey Rep. 2014;3:481.
2. Parfitt AM. Targeted and nontargeted bone remodeling: relationship to basic multicellular unit origination and progression. Bone. 2002;30(1):5-7.
3. Nakashima T, Hayashi M, Fukunaga T, Kurata K, Oh-Hora M, Feng JQ, et al. Evidence for osteocyte regulation of bone homeostasis through RANKL expression. Nat Med. 2011;17(10):1231-4.
4. Kong YY, Feige U, Sarosi I, Bolon B, Tafuri A, Morony S, et al. Activated T cells regulate bone loss and joint destruction in adjuvant arthritis through osteoprotegerin ligand. Nature. 1999;402(6759):304-9.
5. Takahashi N, Akatsu T, Udagawa N, Sasaki T, Yamaguchi A, Moseley JM, et al. Osteoblastic cells are involved in osteoclast formation. Endocrinology. 1988;123(5):2600-2.
6. Martin TJ, Sims NA. Osteoclast-derived activity in the coupling of bone formation to resorption. Trends Mol Med. 2005;11(2):76-81.
7. Irie A, Takami M, Kubo H, Sekino-Suzuki N, Kasahara K, Sanai Y. Heparin enhances osteoclastic bone resorption by inhibiting osteoprotegerin activity. Bone. 2007;41(2):165-74.
8. Walenga JM, Bick RL. Heparin-induced thrombocytopenia, paradoxical thromboembolism, and other side effects of heparin therapy. Med Clin North Am. 1998;82(3):635-58.
9. Kram V, Zcharia E, Yacoby-Zeevi O, Metzger S, Chajek-Shaul T, Gabet Y, et al. Heparanase is expressed in osteoblastic cells and stimulates bone formation and bone mass. J Cell Physiol. 2006;207(3):784-92.
10. Nozawa S, Inubushi T, Irie F, Takigami I, Matsumoto K, Shimizu K, et al. Osteoblastic heparan sulfate regulates osteoprotegerin function and bone mass. JCI Insight. 2018;3(3).
11. Theoleyre S, Kwan Tat S, Vusio P, Blanchard F, Gallagher J, Ricard-Blum S, et al. Characterization of osteoprotegerin binding to glycosaminoglycans by surface plasmon resonance: role in the interactions with receptor activator of nuclear factor kappaB ligand (RANKL) and RANK. Biochemical and biophysical research communications. 2006;347(2):460-7.
12. Benad-Mehner P, Thiele S, Rachner TD, Gobel A, Rauner M, Hofbauer LC. Targeting syndecan-1 in breast cancer inhibits osteoclast functions through up-regulation of osteoprotegerin. J Bone Oncol. 2014;3(1):18-24.
13. Velasco CR, Colliec-Jouault S, Redini F, Heymann D, Padrines M. Proteoglycans on bone tumor development. Drug Discov Today. 2010;15(13-14):553-60.
14. Li M, Yang S, Xu D. Heparan Sulfate Regulates the Structure and Function of Osteoprotegerin in Osteoclastogenesis. J Biol Chem. 2016;291(46):24160-71.
15. Rapraeger A, Jalkanen M, Endo E, Koda J, Bernfield M. The cell surface proteoglycan from mouse mammary epithelial cells bears chondroitin sulfate and heparan sulfate glycosaminoglycans. J Biol Chem. 1985;260(20):11046-52.
16. Sanderson RD, Yang Y, Suva LJ, Kelly T. Heparan sulfate proteoglycans and heparanase--partners in osteolytic tumor growth and metastasis. Matrix Biol. 2004;23(6):341-52.
17. Dhodapkar MV, Abe E, Theus A, Lacy M, Langford JK, Barlogie B, et al. Syndecan-1 is a multifunctional regulator of myeloma pathobiology: control of tumor cell survival, growth, and bone cell differentiation. Blood. 1998;91(8):2679-88.
18. Bernfield M, Hinkes MT, Gallo RL. Developmental expression of the syndecans: possible function and regulation. Development (Cambridge, England). 1993:205-12.
19. Teng YH, Aquino RS, Park PW. Molecular functions of syndecan-1 in disease. Matrix Biol. 2012;31(1):3-16.
20. Stepp MA, Gibson HE, Gala PH, Iglesia DD, Pajoohesh-Ganji A, Pal-Ghosh S, et al. Defects in keratinocyte activation during wound healing in the syndecan-1-deficient mouse. Journal of cell science. 2002;115(Pt 23):4517-31.

21. Bertrand J, Stange R, Hidding H, Echtermeyer F, Nalesso G, Godmann L, et al. Bone fracture repair, but not fetal skeletal development is supported by syndecan-4. Arthritis and rheumatism. 2012.
22. Joensuu H, Anttonen A, Eriksson M, Makitaro R, Alfthan H, Kinnula V, et al. Soluble syndecan-1 and serum basic fibroblast growth factor are new prognostic factors in lung cancer. Cancer Res. 2002;62(18):5210-7.
23. Conejo JR, Kleeff J, Koliopanos A, Matsuda K, Zhu ZW, Goecke H, et al. Syndecan-1 expression is up-regulated in pancreatic but not in other gastrointestinal cancers. Int J Cancer. 2000;88(1):12-20.
24. Keffer J, Probert L, Cazlaris H, Georgopoulos S, Kaslaris E, Kioussis D, et al. Transgenic mice expressing human tumour necrosis factor: a predictive genetic model of arthritis. The EMBO journal. 1991;10(13):4025-31.
25. Dempster DW, Compston JE, Drezner MK, Glorieux FH, Kanis JA, Malluche H, et al. Standardized nomenclature, symbols, and units for bone histomorphometry: a 2012 update of the report of the ASBMR Histomorphometry Nomenclature Committee. J Bone Miner Res. 2013;28(1):2-17.
26. Bouxsein ML, Boyd SK, Christiansen BA, Guldberg RE, Jepsen KJ, Muller R. Guidelines for assessment of bone microstructure in rodents using micro-computed tomography. J Bone Miner Res. 2010;25(7):1468-86.
27. Stange R, Kronenberg D, Timmen M, Everding J, Hidding H, Eckes B, et al. Age-related bone deterioration is diminished by disrupted collagen sensing in integrin alpha2beta1 deficient mice. Bone. 2013;56(1):48-54.
28. Hof CIaRJvt. Osteoclast Formation in Mouse Co-cultures. In: Ralston MHHaSH, editor. Bone Research Protocols, Methods in Molecular Biology. 816. 2 ed: Springer Science and Business Media; 2012. p. 177-86.
29. Yasuda H, Shima N, Nakagawa N, Yamaguchi K, Kinosaki M, Mochizuki S, et al. Osteoclast differentiation factor is a ligand for osteoprotegerin/osteoclastogenesis-inhibitory factor and is identical to TRANCE/RANKL. Proceedings of the National Academy of Sciences of the United States of America. 1998;95(7):3597-602.
30. El Khassawna T, Merboth F, Malhan D, Bocker W, Daghma DES, Stoetzel S, et al. Osteocyte Regulation of Receptor Activator of NF-kappaB Ligand/Osteoprotegerin in a Sheep Model of Osteoporosis. The American journal of pathology. 2017;187(8):1686-99.
31. Malhan D, Muelke M, Rosch S, Schaefer AB, Merboth F, Weisweiler D, et al. An Optimized Approach to Perform Bone Histomorphometry. Front Endocrinol (Lausanne). 2018;9:666.
32. Mansouri R, Jouan Y, Hay E, Blin-Wakkach C, Frain M, Ostertag A, et al. Osteoblastic heparan sulfate glycosaminoglycans control bone remodeling by regulating Wnt signaling and the crosstalk between bone surface and marrow cells. Cell Death Dis. 2017;8(6):e2902.
33. Standal T, Seidel C, Hjertner O, Plesner T, Sanderson RD, Waage A, et al. Osteoprotegerin is bound, internalized, and degraded by multiple myeloma cells. Blood. 2002;100(8):3002-7.
34. Hofbauer LC, Heufelder AE. Role of receptor activator of nuclear factor-kappaB ligand and osteoprotegerin in bone cell biology. J Mol Med (Berl). 2001;79(5-6):243-53.
35. Udagawa N, Takahashi N, Jimi E, Matsuzaki K, Tsurukai T, Itoh K, et al. Osteoblasts/stromal cells stimulate osteoclast activation through expression of osteoclast differentiation factor/RANKL but not macrophage colony-stimulating factor: receptor activator of NF-kappa B ligand. Bone. 1999;25(5):517-23.
36. Boyle WJ, Simonet WS, Lacey DL. Osteoclast differentiation and activation. Nature. 2003;423(6937):337-42.
37. Manolagas SC, Jilka RL. Bone marrow, cytokines, and bone remodeling. Emerging insights into the pathophysiology of osteoporosis. N Engl J Med. 1995;332(5):305-11.

Tables

Table 1: Ingredients of culture medium for osteoblasts, osteoclasts and co-cultures

Table 2: Primers used for quantitative real time PCR

Figure Legends

Figure 1: Syndecan-1 concentration in serum of mice increases with age. Serum of 4, 12 and 18 month old mice (wild type) was collected. Concentration of soluble Syndecan-1 was determined by ELISA. Data are displayed as mean ± SD, Kruskal-Wallis test with Dunn´s post hoc test, n =9-13 per group. *p < 0.05

Figure 2: Bone structure of Syndecan-1 deficient mice during aging. Lumbar vertebrae of mice (wild type, Syndecan-1-/-) at the age of 4, 12 and 18 month were isolated and bone structure was assessed by µCT. Representative pictures of fifth lumbar vertebrae of each age group are shown in A, bone volume/tissue volume (BV/TV) of the trabecular bone in the vertebra body is shown in B. See table 3 for additional bone parameters. Data are displayed as mean ± SD, Kruskal-Wallis test with Dunn´s post hoc test, n =6-10 per group. *p < 0.05, **p<0.01

Figure 3: Expression of Syndecan-1 in osteoblasts and osteoclasts during differentiation in vitro.. Co-cultures of osteoblasts and osteoclasts were performed in presence of $1,25(OH)_2D_3$ and PGE2 (DM+, see Table 1). AB: mRNA expression of Syndecan-1-4 were analysed using quantitative realtime PCR (Primers see Table 2) normalized to HPRT and day 1 of culture ($\Delta\Delta$CT method). C: Protein expression of Syndecan-1 in the cells was detected using a polyclonal antibody against Syndecan-1. Scale bar: 50µm. D: Syndecan-1 expression was analysed after stimulation of osteoblastic cells with DM+ medium. mRNA expression was determined by realtime PCR (left). The concentration of soluble Syndecan-1 protein in the supernatant of cells was analysed by ELISA (right). E: RANKL and OPG expression and protein release into the

supernatant is determined using osteoblasts (WT or Syndecan-1-/-) cultured in DM or DM+ medium. Experiments were performed in independent triplicates (A; B, E) or duplicates (D), data are displayed as mean ± SD.

Figure 4: Differentiation and functionality of osteoblasts and osteoclasts dependent on Syndecan-1. A: Primary osteoblast precursors (WT, Syndecan-1-/-) were cultured in DM-Medium (see Table 1) and mineralization of the extracellular matrix was visualised by von Kossa staining and quantified photometrically after alizarin red staining. B: Osteoclast precursor cells were cultured in DM-Medium supplemented with rmM-CSF and RANKL. Resorption was analysed using dentin chips. Differentiation of osteoclasts was determined as the development of TRAP positive, multinucleated cells. Resorption was measured as the area of resorption pits per whole area using digital imaging. Experiments were performed in triplicates, scale bars: Trap staining: 100µm, resorption: 50µm, data were presented as mean ± SD, Mann-Whitney-U test, *$p < 0.05$

Figure 5: Osteoclast differentiation and RANKL/OPG release in co-cultures of osteoblasts and osteoclasts using Syndecan-1 deficient cells. Primary osteoblast ($2x10^4$ cells/well) and osteoclast precursor cells ($4x10^5$ cells/well) were cultured together in DM+-medium (see Table 1) for up to 7 days. Different combinations of genotypes (WT/Sdc1-/-) as depicted were used (OB/OC). A: After 7 days, the osteoblast layer was removed and TRAP staining was performed, scale bar 200µm. Osteoclast number was determined as TRAP positive, multinucleated cells, Quantification in panel B. C: OPG and RANKL concentrations were determined in cell culture supernatant using ELISA. D: RANKL/OPG ratio was calculated. Experiments were performed in independent triplicates, data represent mean ± SD, 2way ANOVA with Bonferroni´s test, *$p < 0.05$, **$p<0.01$, ***$p<0.001$

Figure 6: Local expression of RANKL/OPG in osteocytes of Syndecan-1 deficient bone during aging. Paraffin sections of lumbar vertebra body of 4 and 18 month old wild type or Syndecan-1

deficient mice were stained for RANKL or OPG (A, in red). The slides were counterstained with silver nitrate to visualize calcified bone. Scale bar: 20µm. B: Total osteocyte number positive for RANKL or OPG were counted and normalized to trabecular bone area displayed as mean ± SD. Mann-Whitney-U test, n =5-6 per group. *p < 0.05, **p<0.01. C: Osteoclast number on the trabecular bone surface of vertebra of Syndecan-1 deficient mice during aging. TRAP positive cells on the bone surface of trabeculae were counted and the surface of bone was determined using Cellsense software. Osteoclast number is shown as cell number per mm and displayed as mean ± SD. Kruskal-Wallis test with Dunn´s post hoc test, n =4-15 per group. *p < 0.05, **p<0.01. D: Systemic bone resorption was determined using serum of 4 and 18 month old mice (WT, Syndecan-1-/-) for ELISA to measure carboxy-terminal collagen crosslinks (CTX). Data represent mean ± SD, Holm-Sidak method, n=5-9, *p<0.05

Figure 7: Proposed function of Syndecan-1 in local bone cell communication (model)

Supplemental Data

Supplemental figure 1: Bone development in Syndecan-1 deficient mice. A: Whole skeleton of newborn mice were used for alcian blue/alizarin red staining of bone and cartilage, n=6, scale bar 2 mm. B: Maturation of bone development was quantified as ratio of calcified area per whole bone area [%] in the humerus, femur and tibia of wild type and Syndecan-1 deficient mice. Data presented as mean ± SD. C: Representative pictures of tibia sections of newborn mice stained for cartilage (Alcian blue), calcified bone (Masson-Goldner) as well as collagen II and collagen X using immunohistochemical staining.

Supplemental table 1: Bone parameters of wild type and Syndecan-1 deficient mice during aging Bone structure was assessed by µCT in vertebra of 4 to 18 month old female Syndecan-1 deficient and wild type mice. Data are presented as mean ± SD, n = 6–10 per group. TV = Tissue volume; BV/TV = bone volume fraction; Tb.N = trabecular number; Tb.Th = trabecular thickness; Tb.Sp = trabecular separation; Ct.Th = cortical thickness. Kruskal-Wallis test with Dunn´s post

hoc test, n =9-13 per group. * indicate significant difference within age matched genotypes: no significant differences found, # indicate significant difference to 4 month old group of the same genotype, #p>0.05, ##p>0.01, ###p>0.001, ####p>0.00001

Supplemental Figure 2: Titration of OPG in RANKL-ELISA measurement. RANKL concentration was determined in presence of different OPG concentrations using a RANKL ELISA assay (here R&D). We could show that OPG interferes with the detection of RANKL in this measurements. To our knowledge there is no RANKL ELISA available that detects RANKL bound to OPG.

Supplemental Figure 3: mRNA expression of RANK, RANKL and OPG in osteoblasts and osteoclasts dependent on Syndecan-1. Primary bone cell precursor cells from mice (WT, Syndecan-1-/-) (OB, OC) were cultured separately or in co-culture (OB/OC). mRNA was isolated after up to 25 days as depicted in the graphs and expression of RANK, RANKL and OPG was determined normalized to HPRT using quantitative realtime PCR. Experiments were performed three times, in triplicates, data were presented as mean ± SD.

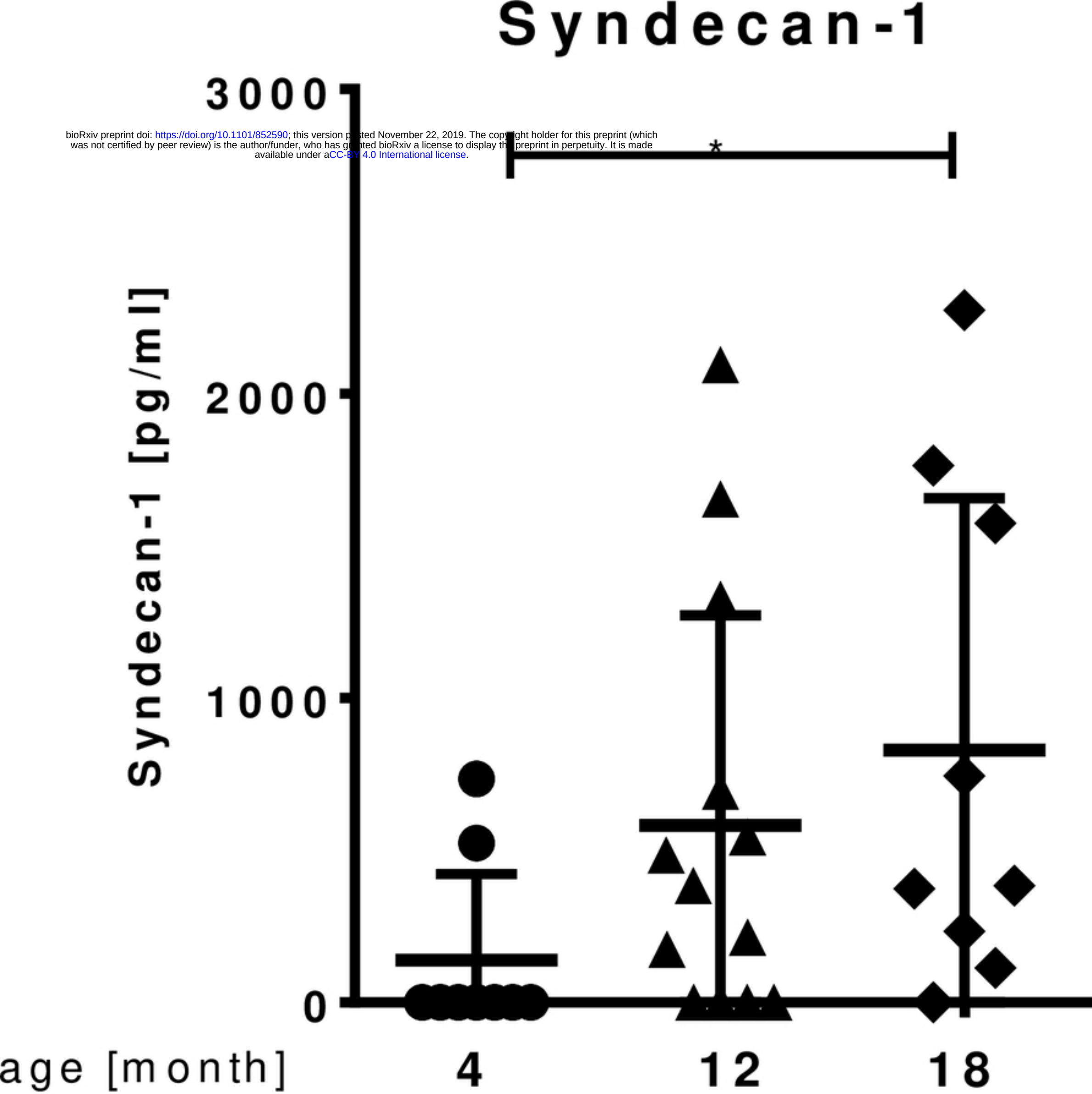

Figure 1

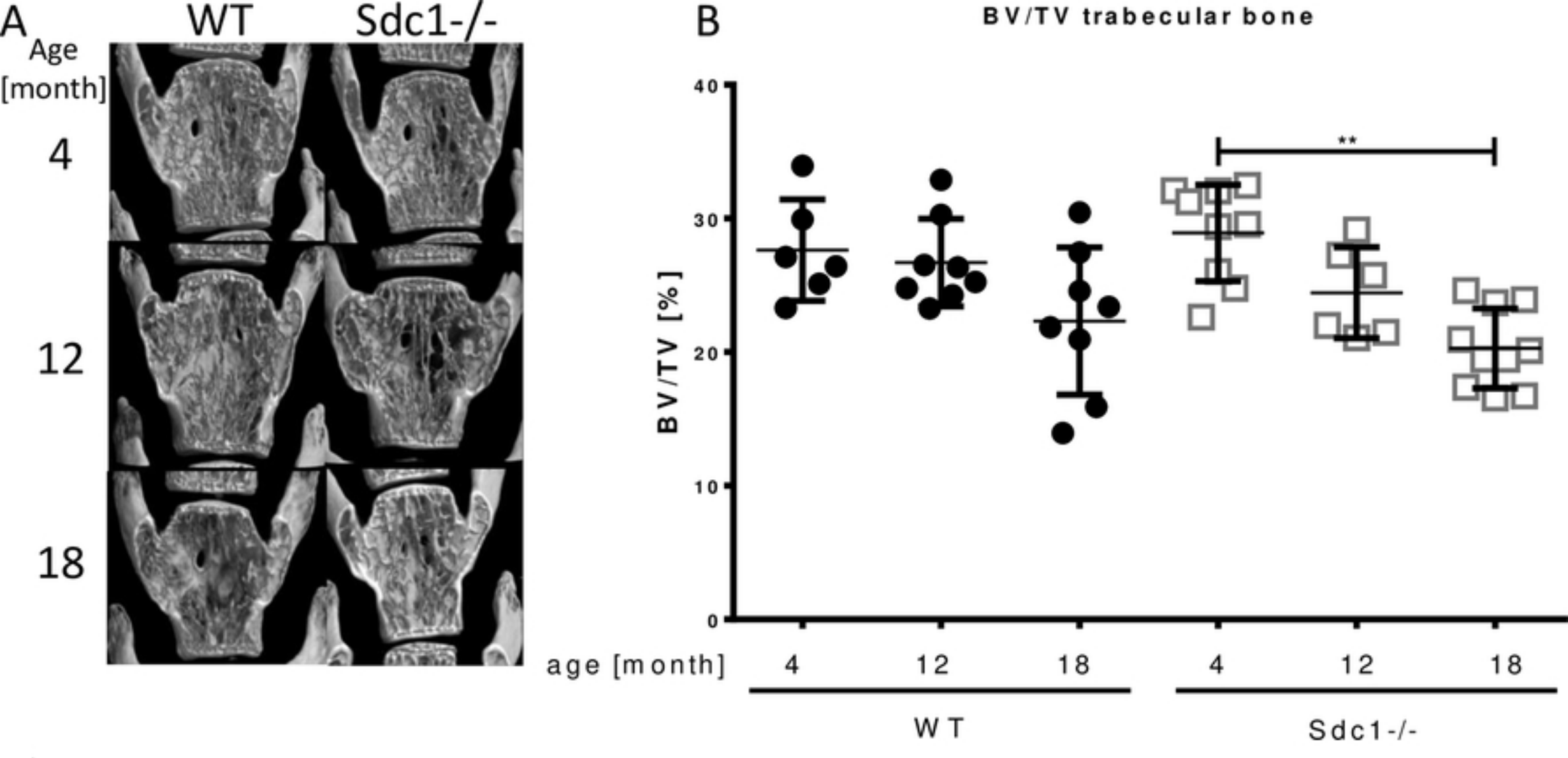
A
WT
Sdc1-/-
Age [month]
4
12
18
B
BV/TV trabecular bone
BV/TV [%]
40
30
20
10
0
**
age [month]
4
12
18
4
12
18
WT
Sdc1-/-

Figure 2

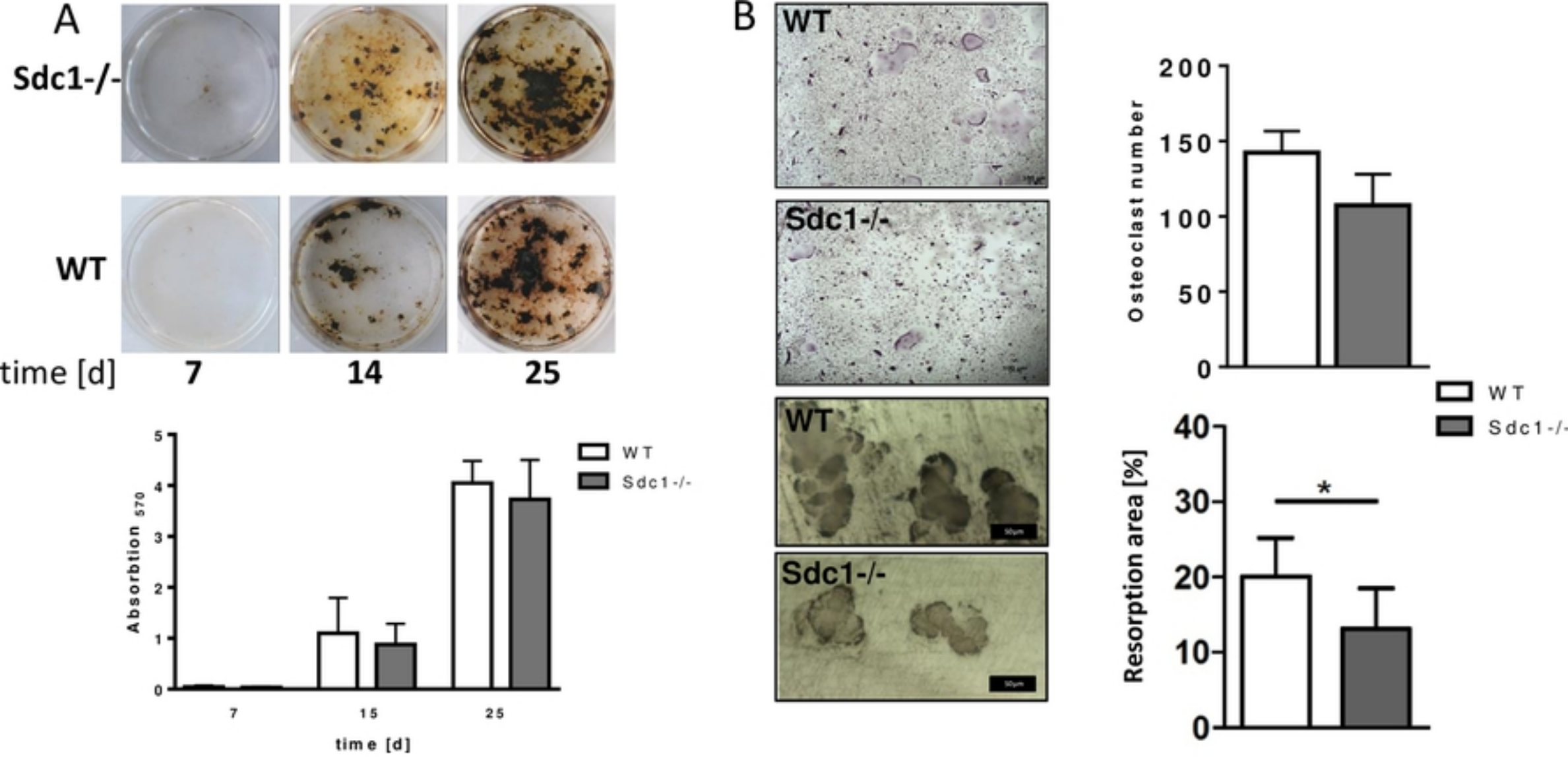
A
Sdc1-/-
WT
time [d]
7
14
25
Absorbtion 570
WT
Sdc1-/-
time [d]
B
WT
Sdc1-/-
WT
Sdc1-/-
Osteoclast number
Resorption area [%]
*

Figure 4

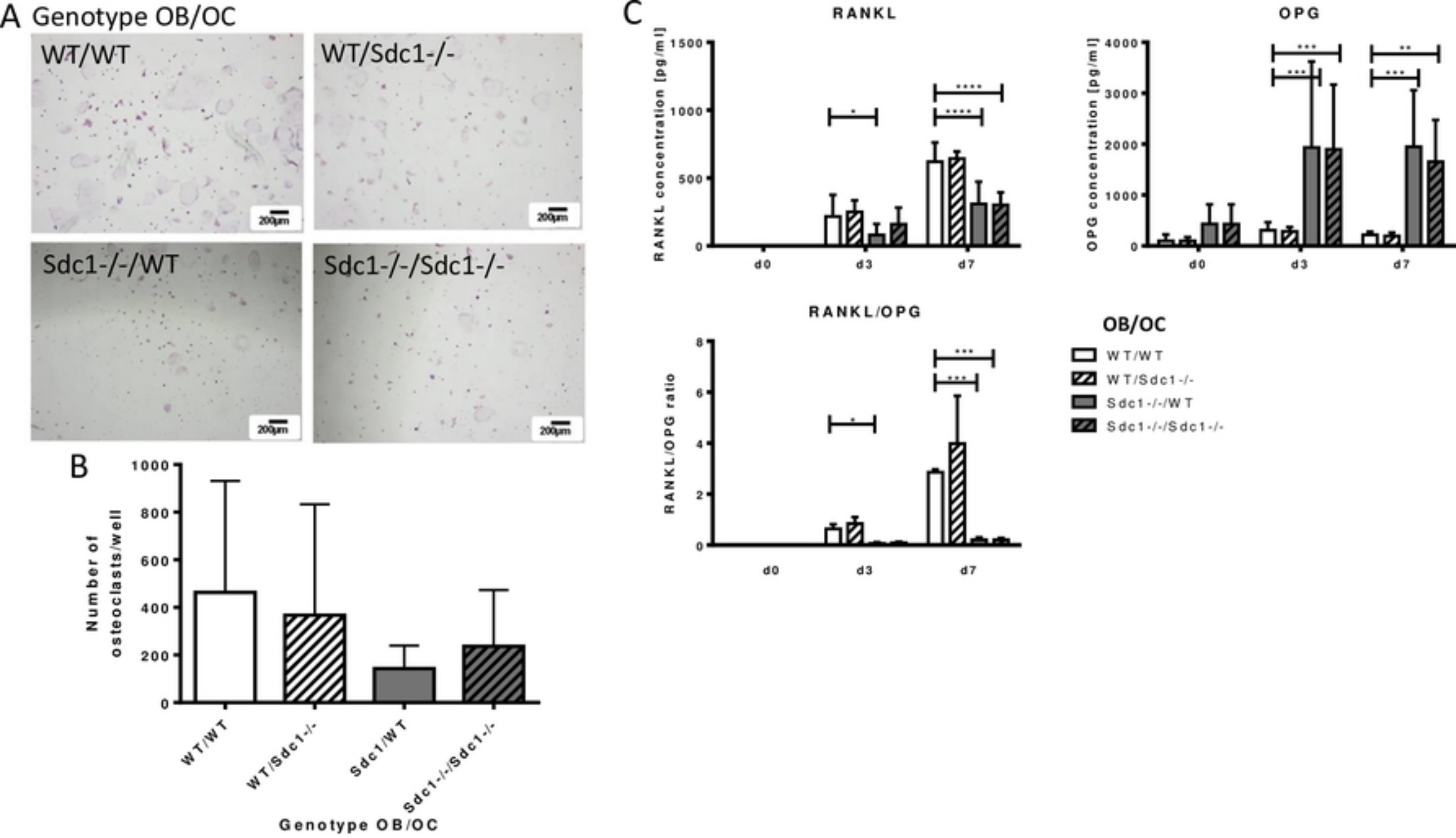
A Genotype OB/OC
WT/WT
WT/Sdc1-/-
Sdc1-/-/WT
Sdc1-/-/Sdc1-/-
200µm
B
Number of osteoclasts/well
1000
800
600
400
200
0
WT/WT
WT/Sdc1-/-
Sdc1/WT
Sdc1-/-/Sdc1-/-
Genotype OB/OC
C
RANKL
RANKL concentration [pg/ml]
1500
1000
500
0
d0
d3
d7
OPG
OPG concentration [pg/ml]
4000
3000
2000
1000
0
RANKL/OPG
RANKL/OPG ratio
8
6
4
2
0
OB/OC
WT/WT
WT/Sdc1-/-
Sdc1-/-/WT
Sdc1-/-/Sdc1-/-

Figure 5

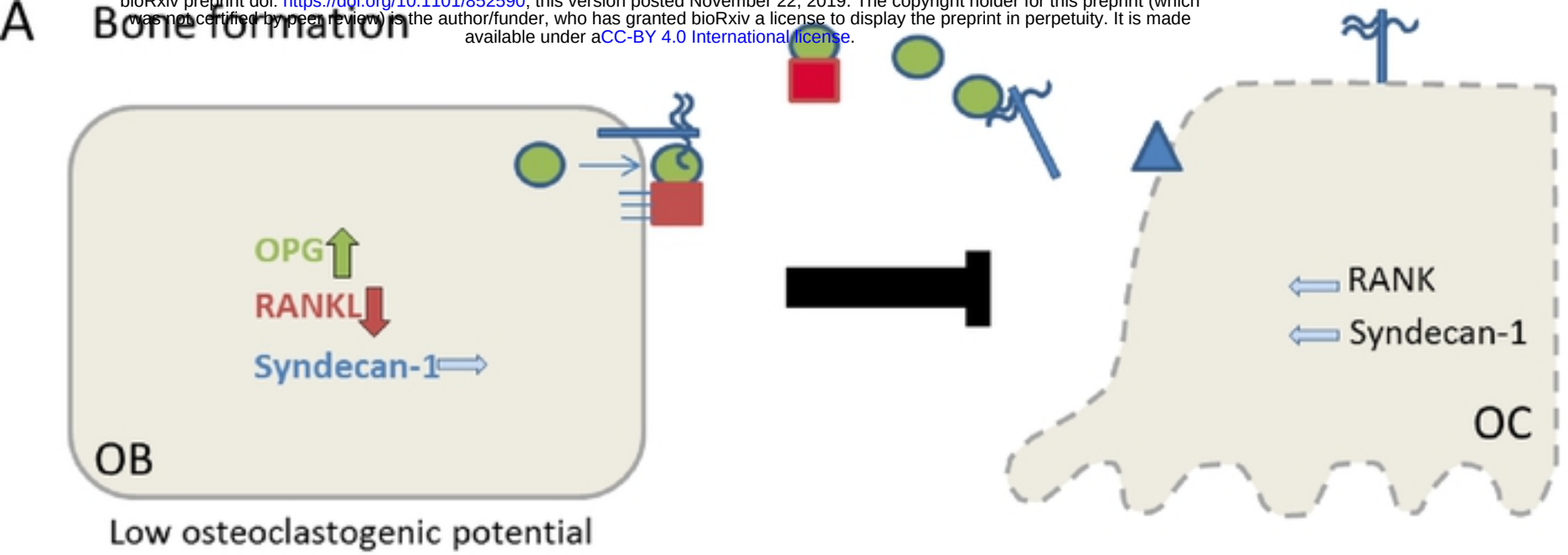

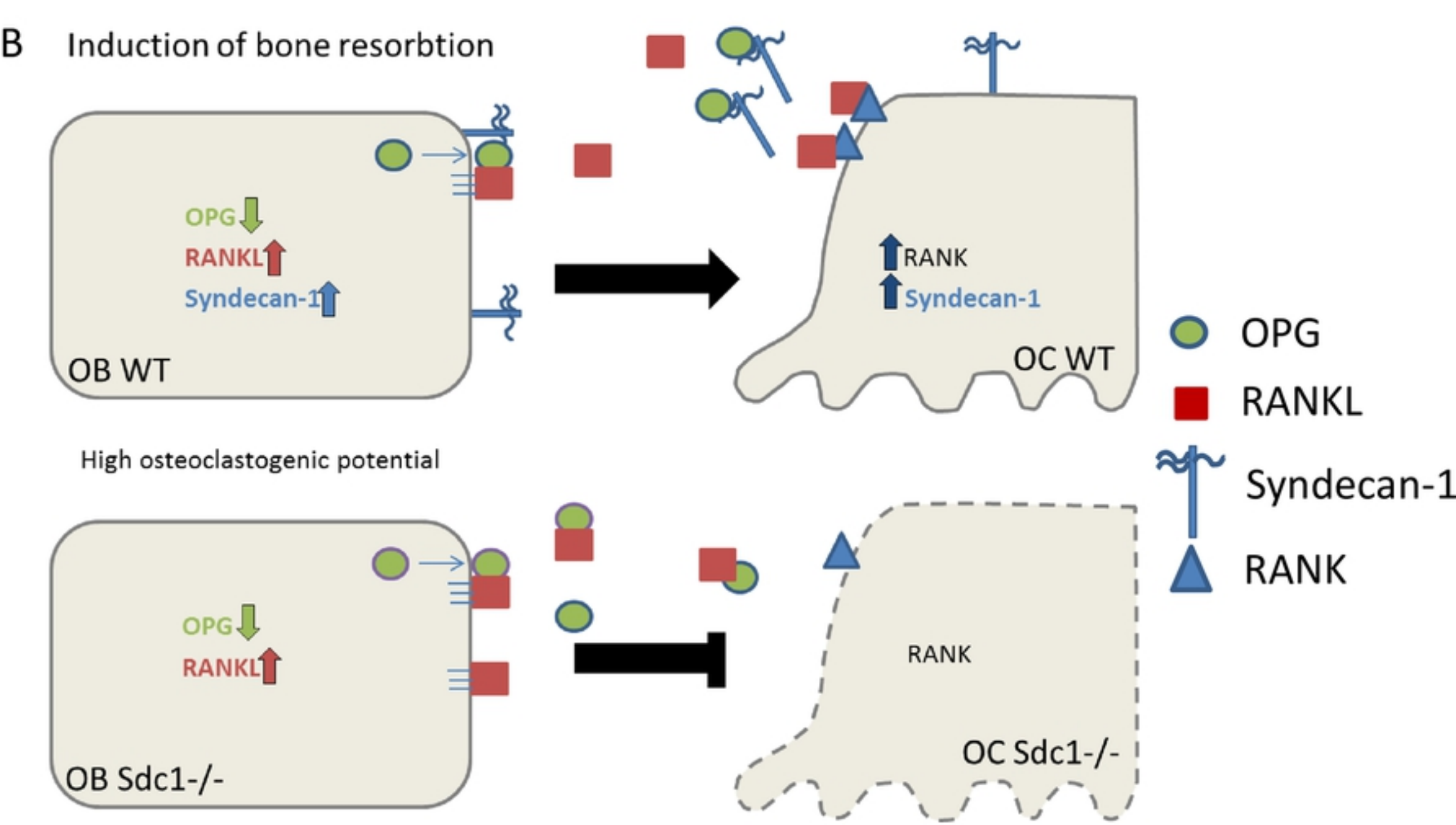

Figure 7

Medium	Ingredients
Basal	Alpha-MEM, 10 % FCS, 2 mM L-glutamine penicillin (100 U/ml)/streptomycin (100 µg/ml)
DM	Basal plus 0.2 mM L-ascorbic acid 2-phosphate, 10 mM beta-glycerol phosphate,
DM+	DM plus 1 µM PGE2, 10 nM $1,25(OH)_2D_3$

Table 1

Name (*gene*)	**forward**	**reverse**
Syndecan-1 (*sdc1*)	tctggggatgactctgacaac	tgccgtgacaaagtatctgg
Syndecan-2 (*sdc2*)	ttcaggagtatatcctattgatgatga	actctctatgtcttcatcagctcct
Syndecan-3 (*sdc3*)	cagctccctcagaagagcat	acccacgatcacggctac
Syndecan-4 (*sdc4*)	cccttccctgaagtgattga	agttccttgggctctgagg
RANK (*Tnfrsf11a*)	gtgctgctcgttccactg	agatgctcataatgcctctcct
RANKL (*Tnfsf11*)	ggccacagcgcttctcag	gagtgactttatgggaacccgat
OPG (*Tnfrsf11b*)	gtttcccgaggaccacaat	ccattcaatgatgtccaggag
HPRT (*Hprt*)	tgatagatccattcctatgactgtaga	aagacattctttccagttaaagttgag

Table 2

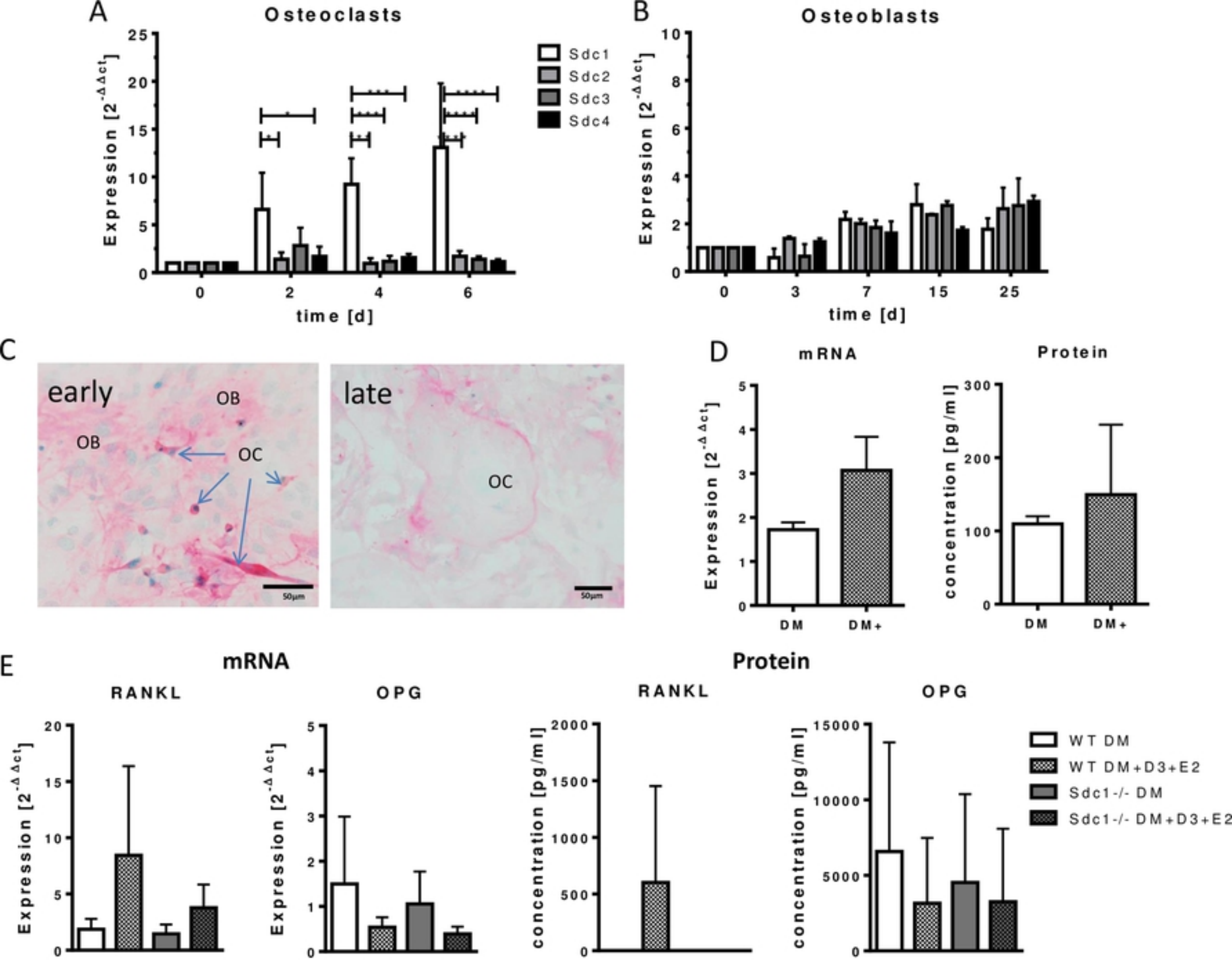
A
Osteoclasts
Expression [2^-ΔΔct]
time [d]
Sdc1
Sdc2
Sdc3
Sdc4
B
Osteoblasts
Expression [2^-ΔΔct]
time [d]
C
early
OB
OB
OC
50µm
late
OC
50µm
D
mRNA
Protein
Expression [2^-ΔΔct]
concentration [pg/ml]
DM
DM+
E
mRNA
Protein
RANKL
OPG
RANKL
OPG
Expression [2^-ΔΔct]
concentration [pg/ml]
WT DM
WT DM+D3+E2
Sdc1-/- DM
Sdc1-/- DM+D3+E2

Figure 3

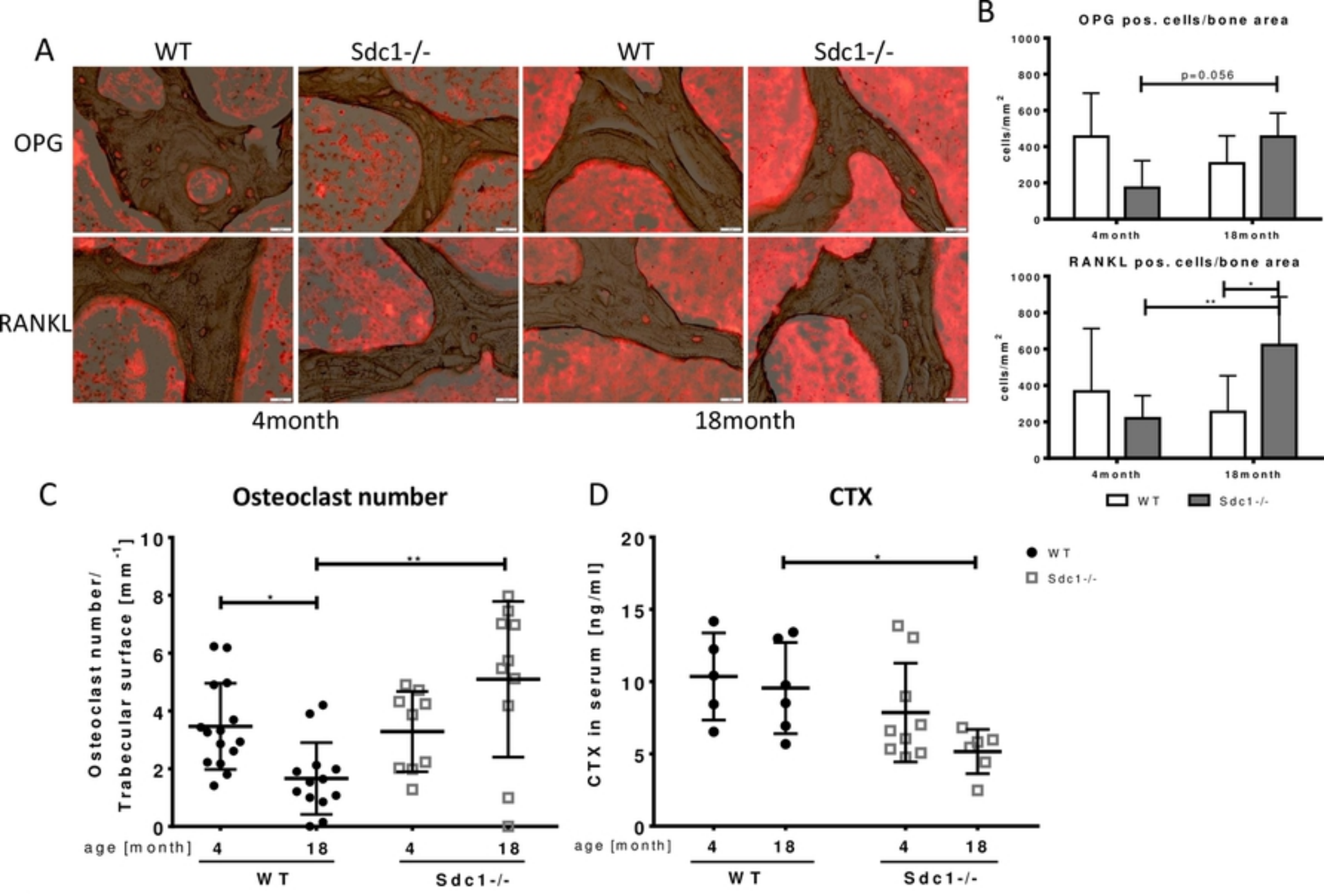
A
WT
Sdc1-/-
WT
Sdc1-/-
OPG
RANKL
4month
18month
B
OPG pos. cells/bone area
cells/mm²
p=0.056
4month
18month
RANKL pos. cells/bone area
cells/mm²
*
**
4month
18month
WT
Sdc1-/-
C
Osteoclast number
Osteoclast number/ Trabecular surface [mm⁻¹]
*
**
age [month]
4
18
4
18
WT
Sdc1-/-
D
CTX
CTX in serum [ng/ml]
*
WT
Sdc1-/-
age [month]
4
18
4
18
WT
Sdc1-/-

Figure 6